Supporting information

Photochemical and Gas Adsorption Studies of Keggin Polyoxometalate Functionalized Porous Melamine Terphthaldehyde Material

*Anjali Tripathi and Sabbani Supriya**

School of Physical Sciences, Jawaharlal Nehru University, New Delhi-110067, India

SECTION 1	Experimental section	2-3
SECTION 2	Elemental (CHN) analysis	4
SECTION 3	ICP studies	4-7
SECTION 4	Thermogravimetric analysis(TGA)	8-11
SECTION 5	Scanning electron microscopy (SEM)	12-16
SECTION 6	EDAX analysis	17
SECTION 7	BET DATA	18-20
SECTION 8	Comparision of gas adsorption data with literature reported system	21-24
SECTION 9	DFT calculation with ORCA	25-32

1. EXPERIMENTAL SECTION

Materials and Methods

Bruker Model EMX MicroX Spectrometer on fixed frequency mode (X band spectroscope) was used to record the ESR spectra of the compound in solid-state at room temperature. To record the IR spectra, Shimadzu IR Affinity - 1S spectrometer is used. Attenuated total reflection mode *i.e.,* ATR mode was used to analyze the solid-state samples. The background scan of the air is recorded before measuring the spectrum of the compound. Diffused reflectance spectra (DRS) are recorded on Shimadzu UV 2600 UV-vis spectrophotometer in a wavelength range of 220-1400 nm. The powder X-ray diffraction measurements for all the compounds are performed on Rigaku (miniflex-600) Powder X-ray diffractometer (functioning in Bragg-Brentano geometry) with CuKα_1 radiation (λ = 1.54059 Å) in the range of 5 to 40^o (2θ) with 2^o per minute scan rate. performed on Rigaku (miniflex-600) Powder X-ray diffractometer. The sample was prepared on the glass sample holder by overlaying finely divided powder of the compounds. The thermogravimetric analysis data are collected on a Mettler-Toledo (model TGA 1) with a preinstalled Mini chiller MT/230 in temperature window of 25^o - 800 ^{o}C at the scale of 5^o per minute providing dry nitrogen gas with the flow rate of 20 cm^3 per minute. Prior to recording the data for the solid sample, a blank experiment was run under the same parameters using an empty ceramic crucible. The data were analyzed using STARe software V13.00. A standard three electrode system is employed in Na_2SO_4 electrolyte solution consisting of an Ag/AgCl reference electrode, a Pt wire as a counter electrode, and glassy carbon electrode as a working electrode. The morphology and elemental composition of compounds are analyzed by scanning electron microscopy (SEM) equipped with an energy dispersive spectroscope (EDX) using a Zeiss EVO40 instrument. The percentage mass of the Mo in Keggin loaded POM@PMTR composites is determined using an inductive coupled plasma optical emission spectrometer (ICP-OES, Agilent- 5110). Elemental analysis is performed using Vario Micro Cube V4.0.11 CHNS analyser. BET isotherm: Gas physisorption experiments and micropore analysis were conducted at 77 K and 298 K using an Autosorb-iQ from Anton Paar Quanta Tec Inc. Before sorption measurements, the samples are degassed in vacuum overnight at 120 °C. (Hydrogen and carbon dioxide physisorption experiments were performed at 77 K and 298 K respectively). Density functional theory calculations are performed within the framework of DFT, by using the projector augmented wave method as implemented in the Vienna ab Initio Simulation Package.

Synthesis

Synthesis of Compound 1-3$_{red}$:

The yellow color composites **1**, **2**, **3** on irradiated with sunlight for 20, 15, and 10 minutes respectively are converted into dark blue color compounds.

Compound 1$_{red}$ - IR: *3100-3300 (C-H),1543 (C-N), 1479 (C-N), 1348, 1060 (P-O), 1012, 962 (v(Mo=O), 874 (v(Mo-O-Mo)), 807*

Compound 2$_{red}$- *IR: 3100-3300, (C-H, 1540 (C-N), 1469 (C-N), 1345, 1062 (P-O), 1009(), 964 (v(Mo-O), 874 (v(Mo-O-Mo),807,*

Compound 3$_{red}$ - *IR: 3100-3300, (C-H)1537 (C-N), 1469 (C-N), 1350, 1065 (P-O), 1011, 963 (v(Mo-O), 875 (v(Mo-O-Mo), 804*

IR **Compound 1-$_{reg}$:***IR: 3100-3300 (C-H), 1542 (C-N), 1478 (C-N), 1348, 1061 (P-O), 1012, 964 (v(Mo=O), 874 (v(Mo-O-Mo)) ,807*

Compound 2-$_{reg}$: IR:*3100-3300 (C-H), 1540 (C-N), 1469 (C-N), 1347, 1061 (P-O), 1009(), 963 (v(Mo-O), 874 (v(Mo-O-Mo), 805,*

Compound 3-$_{reg}$: IR: *3100-3300 (C-H),1538 (C-N), 1472(C-N), 1350, 1065 (P-O), 1010, 963 (v(Mo-O), 876 (v(Mo-O-Mo), 804*

2. Elemental Analysis

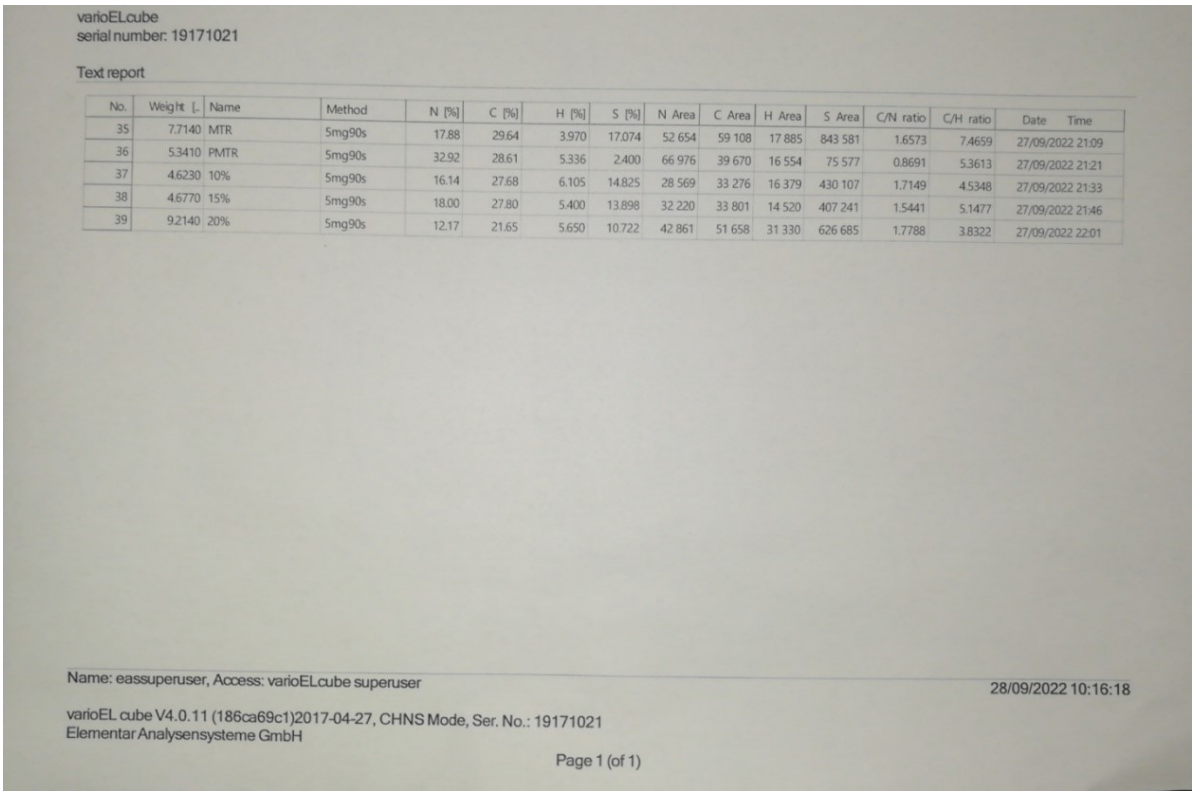

varioELcube
serial number: 19171021

Text report

No.	Weight [..	Name	Method	N [%]	C [%]	H [%]	S [%]	N Area	C Area	H Area	S Area	C/N ratio	C/H ratio	Date Time
35	7.7140	MTR	5mg90s	17.88	29.64	3.970	17.074	52 654	59 108	17 885	843 581	1.6573	7.4659	27/09/2022 21:09
36	5.3410	PMTR	5mg90s	32.92	28.61	5.336	2.400	66 976	39 670	16 554	75 577	0.8691	5.3613	27/09/2022 21:21
37	4.6230	10%	5mg90s	16.14	27.68	6.105	14.825	28 569	33 276	16 379	430 107	1.7149	4.5348	27/09/2022 21:33
38	4.6770	15%	5mg90s	18.00	27.80	5.400	13.898	32 220	33 801	14 520	407 241	1.5441	5.1477	27/09/2022 21:46
39	9.2140	20%	5mg90s	12.17	21.65	5.650	10.722	42 861	51 658	31 330	626 685	1.7788	3.8322	27/09/2022 22:01

Name: eassuperuser, Access: varioELcube superuser
28/09/2022 10:16:18

varioEL cube V4.0.11 (186ca69c1)2017-04-27, CHNS Mode, Ser. No.: 19171021
Elementar Analysensysteme GmbH

Page 1 (of 1)

Fig. S1 CHN elemental analysis of MTR, PMTR and compounds **1**, **2** and **3**.

3. ICP studies

Based on the experimental ICP analysis, we have calculated the amount of Keggin present in compounds **1**, **2** and **3**. The experimental ICP data for molybdenum is summarized in table S1. For compound **1** (10 wt % Keggin loaded PMTR), the amount of molybdenum calculated from ICP analysis is 0.0621 g per 100 g of sample. Therefore, 0.09845 g of Keggin [$H_3PMo_{12}O_{40}$] is present per 100 g of compounds **1**. For compounds **2** (15 wt % Keggin loaded PMTR) the amount of molybdenum obtained from ICP analysis is 0.080871 g per 100 g of sample. Hence the 100 g of compound contains 0.1282 g of [$H_3PMo_{12}O_{40}$]. The ICP analysis of compound **3** shows that 100 g of compound consists of 0.1444 g of molybdenum which accounts to 0.2289 g of [$H_3PMo_{12}O_{40}$] Keggin per 100g of sample. Therefore, the approximate loading as per ICP analysis is found to be 0.1 wt % for compound **1**, 0.15 wt % for compound **2** and 0.23 wt % for compound **3**.

Table S1. Mo concentration calculation in different wt% loaded POM@PMTR composites from ICP-OES analysis.

Compound	Concentration of Mo (ppm)
1(10 wt% loaded POM@PMTR)	621.00
2 (15 wt% loaded POM@PMTR)	808.71
3 (20 wt% loaded POM@PMTR)	1444.52

Path: D:\ICP_RESULTS\Mohd.Alshali\Heavy metals_02.12.2022.esws

Date created: 12/2/2022 12:17:37 PM

Instrument used: MY18411009

Software Version : 7.4.1.10449

Firmware Version : 3585

Notes:

Drift correct with Argon lines: False

Peak track lines used :

Calibration Correlation Coefficient Limit: 0.999

Standard addition: Off

Reagent Blank: Off

Reslope: Off

Replicates: 3

QC Active: Off

IEC: Off

Oxygen Injection Mode: Off

Sample introduction: Manual

SVS 1 delay (s): N/A

Sample Uptake Time (s): 15

Rinse time (s): N/A

AVS 4 : Off

AVS 4 delay (s): N/A

AVS 6/7 : Off

Uptake Rate (mL/min) : N/A

Inject Rate (mL/min) : N/A

Uptake Delay (s) : N/A

Bubble Injection Time (s) : N/A

Preemptive Rinse time (s) : N/A

Intelligent Rinse enabled: Off

Isomist : Off

Isomist Temperature (°C): N/A

Pump Speed (rpm): 12

Sample uptake fast pump: On

Rinse time fast pump: N/A

Condition Set 1

Read time (s): 5

RF power (kW): 1.2

Stabilization time (s): 15

Viewing mode: Axial

Viewing height (mm): N/A

Nebulizer flow(L/min): 0.7

Plasma flow(L/min): 12

Aux flow(L/min): 1

Make up flow(L/min): 0

Oxygen %: 0

Date Time	Label	Element Label (nm)	Conc	%RSD	Unadjusted Conc
2/13/2023 15:30:30	Sample 53	Mn (257.610 nm)	-0.48 u (ppm)	87.65	-0.48 u (ppm)
2/13/2023 15:30:30	Sample 53	Mo (202.032 nm)	1801.29 o (ppm)	0.31	1801.29 o (ppm)
2/13/2023 15:30:30	Sample 53	Ni (231.604 nm)	127.26 (ppm)	6.50	127.26 (ppm)
2/13/2023 15:30:30	Sample 53	Pb (220.353 nm)	-4.63 u (ppm)	> 100.00	-4.63 u (ppm)
2/13/2023 15:30:30	Sample 53	Zn (213.857 nm)	32.13 (ppm)	3.00	32.13 (ppm)
2/13/2023 15:47:30	15%POM@PMTR	As (188.980 nm)	-14.68 u (ppm)	> 100.00	-14.68 u (ppm)
2/13/2023 15:47:30	15%POM@PMTR	B (249.772 nm)	-42.92 u (ppm)	5.22	-42.92 u (ppm)
2/13/2023 15:47:30	15%POM@PMTR	Cd (214.439 nm)	-1.10 u (ppm)	> 100.00	-1.10 u (ppm)
2/13/2023 15:47:30	15%POM@PMTR	Co (238.892 nm)	-12.39 u (ppm)	35.64	-12.39 u (ppm)
2/13/2023 15:47:30	15%POM@PMTR	Cr (267.716 nm)	-0.86 u (ppm)	> 100.00	-0.86 u (ppm)
2/13/2023 15:47:30	15%POM@PMTR	Cu (327.395 nm)	7.02 (ppm)	35.09	7.02 (ppm)
2/13/2023 15:47:30	15%POM@PMTR	Ga (294.363 nm)	-23.75 u (ppm)	69.88	-23.75 u (ppm)
2/13/2023 15:47:30	15%POM@PMTR	Mn (257.610 nm)	-0.27 u (ppm)	> 100.00	-0.27 u (ppm)
2/13/2023 15:47:30	15%POM@PMTR	Mo (202.032 nm)	808.71 (ppm)	1.20	808.71 (ppm)
2/13/2023 15:47:30	15%POM@PMTR	Ni (231.604 nm)	125.76 (ppm)	9.76	125.76 (ppm)
2/13/2023 15:47:30	15%POM@PMTR	Pb (220.353 nm)	-18.68 u (ppm)	> 100.00	-18.68 u (ppm)
2/13/2023 15:47:30	15%POM@PMTR	Zn (213.857 nm)	21.41 (ppm)	6.58	21.41 (ppm)
2/13/2023 15:48:36	10%POM@PMTR	As (188.980 nm)	-39.64 u (ppm)	50.15	-39.64 u (ppm)
2/13/2023 15:48:36	10%POM@PMTR	B (249.772 nm)	-43.52 u (ppm)	5.28	-43.52 u (ppm)
2/13/2023 15:48:36	10%POM@PMTR	Cd (214.439 nm)	-1.89 u (ppm)	10.75	-1.89 u (ppm)
2/13/2023 15:48:36	10%POM@PMTR	Co (238.892 nm)	-11.97 u (ppm)	40.75	-11.97 u (ppm)
2/13/2023 15:48:36	10%POM@PMTR	Cr (267.716 nm)	-4.96 u (ppm)	35.15	-4.96 u (ppm)
2/13/2023 15:48:36	10%POM@PMTR	Cu (327.395 nm)	0.16 u (ppm)	> 100.00	0.16 u (ppm)
2/13/2023 15:48:36	10%POM@PMTR	Ga (294.363 nm)	-29.84 u (ppm)	18.40	-29.84 u (ppm)
2/13/2023 15:48:36	10%POM@PMTR	Mn (257.610 nm)	-0.74 u (ppm)	43.64	-0.74 u (ppm)
2/13/2023 15:48:36	10%POM@PMTR	Mo (202.032 nm)	621.00 (ppm)	0.80	621.00 (ppm)
2/13/2023 15:48:36	10%POM@PMTR	Ni (231.604 nm)	122.04 (ppm)	1.65	122.04 (ppm)
2/13/2023 15:48:36	10%POM@PMTR	Pb (220.353 nm)	-11.53 u (ppm)	39.35	-11.53 u (ppm)
2/13/2023 15:48:36	10%POM@PMTR	Zn (213.857 nm)	18.88 (ppm)	3.68	18.88 (ppm)
2/13/2023 15:49:39	20%POM@PMTR	As (188.980 nm)	-6.95 u (ppm)	> 100.00	-6.95 u (ppm)
2/13/2023 15:49:39	20%POM@PMTR	B (249.772 nm)	-39.70 u (ppm)	9.14	-39.70 u (ppm)
2/13/2023 15:49:39	20%POM@PMTR	Cd (214.439 nm)	-2.90 u (ppm)	28.83	-2.90 u (ppm)
2/13/2023 15:49:39	20%POM@PMTR	Co (238.892 nm)	-13.85 u (ppm)	14.52	-13.85 u (ppm)
2/13/2023 15:49:39	20%POM@PMTR	Cr (267.716 nm)	-4.13 u (ppm)	30.84	-4.13 u (ppm)
2/13/2023 15:49:39	20%POM@PMTR	Cu (327.395 nm)	-0.52 u (ppm)	> 100.00	-0.52 u (ppm)
2/13/2023 15:49:39	20%POM@PMTR	Ga (294.363 nm)	-16.19 u (ppm)	96.31	-16.19 u (ppm)
2/13/2023 15:49:39	20%POM@PMTR	Mn (257.610 nm)	-0.62 u (ppm)	65.69	-0.62 u (ppm)
2/13/2023 15:49:39	20%POM@PMTR	Mo (202.032 nm)	1444.52 o (ppm)	0.58	1444.52 o (ppm)
2/13/2023 15:49:39	20%POM@PMTR	Ni (231.604 nm)	120.87 (ppm)	7.80	120.87 (ppm)
2/13/2023 15:49:39	20%POM@PMTR	Pb (220.353 nm)	-13.44 u (ppm)	36.45	-13.44 u (ppm)
2/13/2023 15:49:39	20%POM@PMTR	Zn (213.857 nm)	20.52 (ppm)	0.44	20.52 (ppm)

4. Thermogravimetric analysis

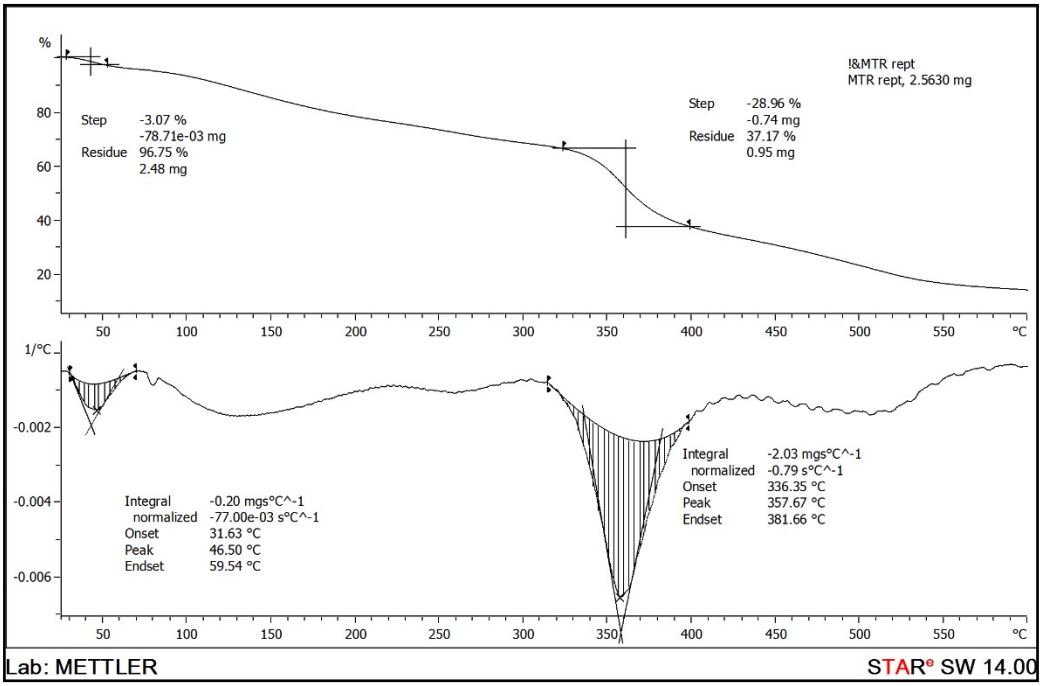

Fig. S2 (a) Thermal analysis plot for MTR.

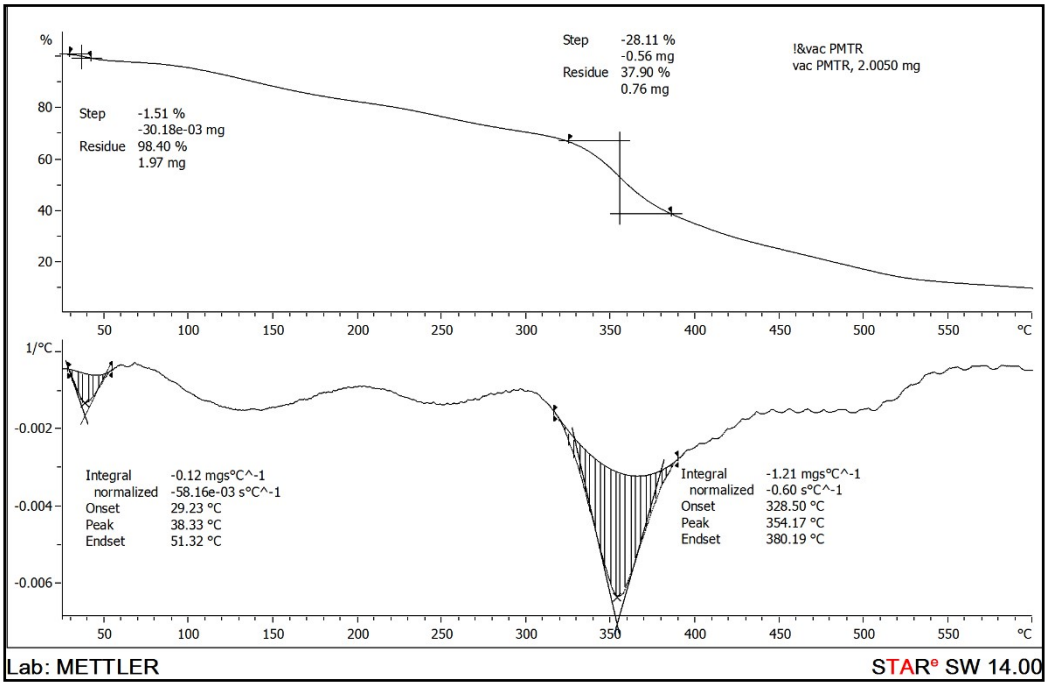

Fig. S2 (b) Thermal analysis plot for PMTR.

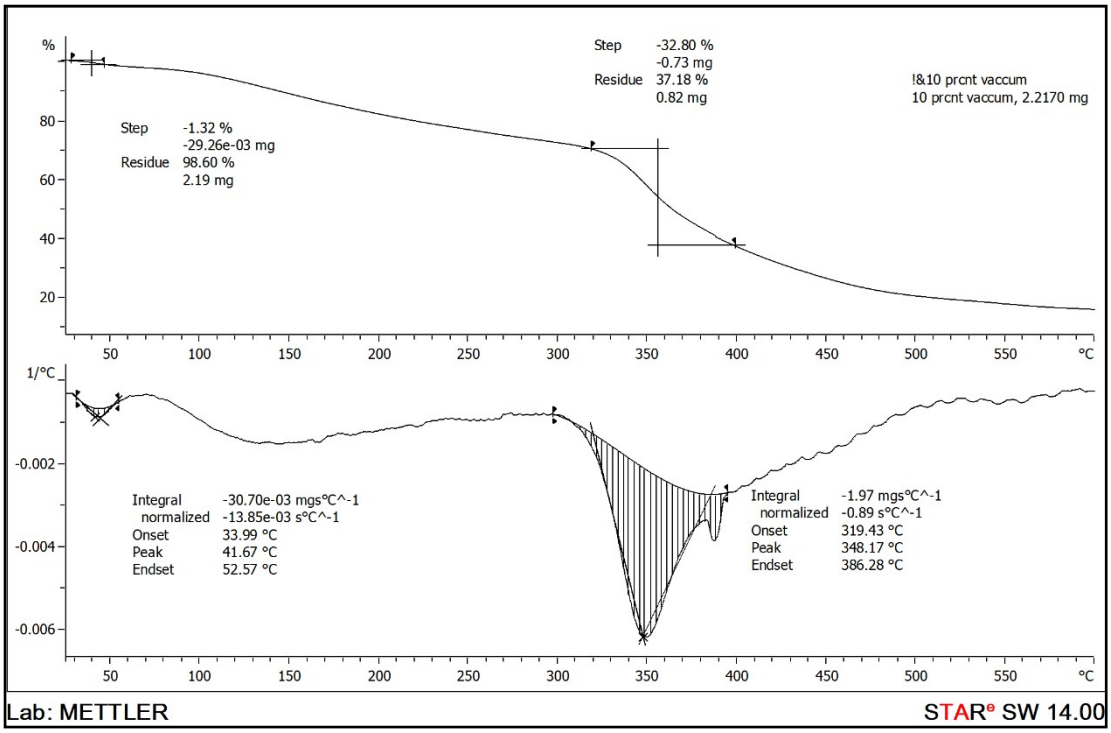

Fig. S2 (c) Thermal analysis plot for Compound **1**.

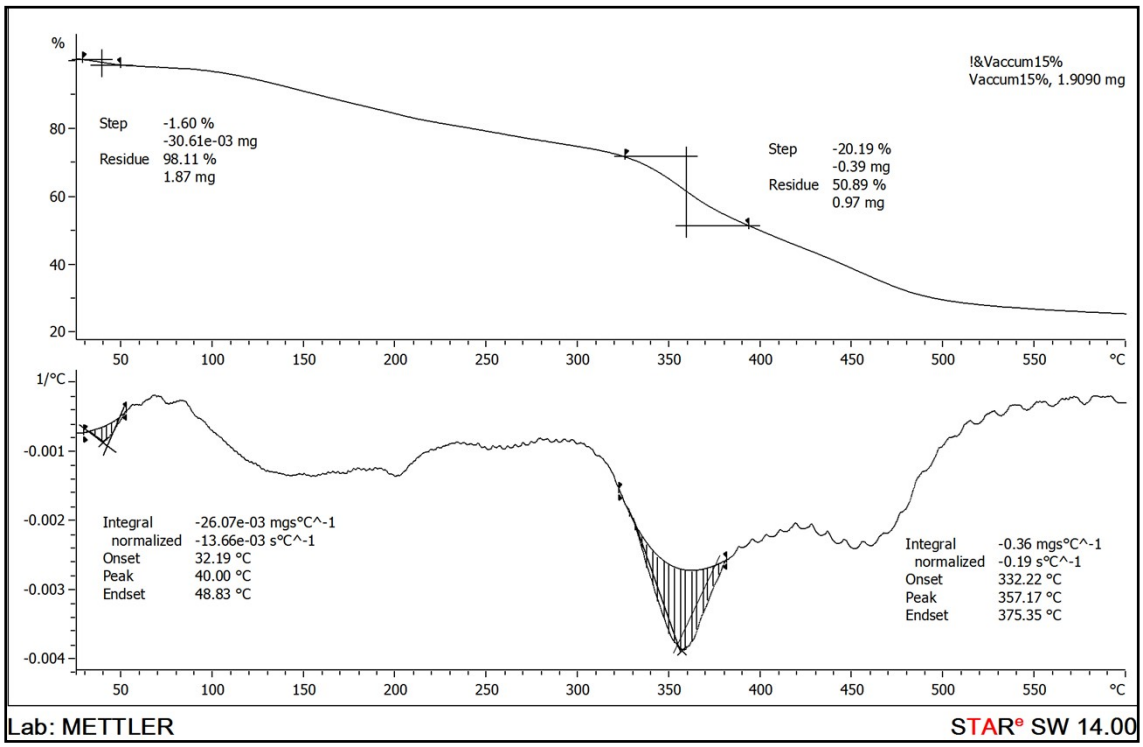

Fig.S2 (d) Thermal analysis plot for compound **2**.

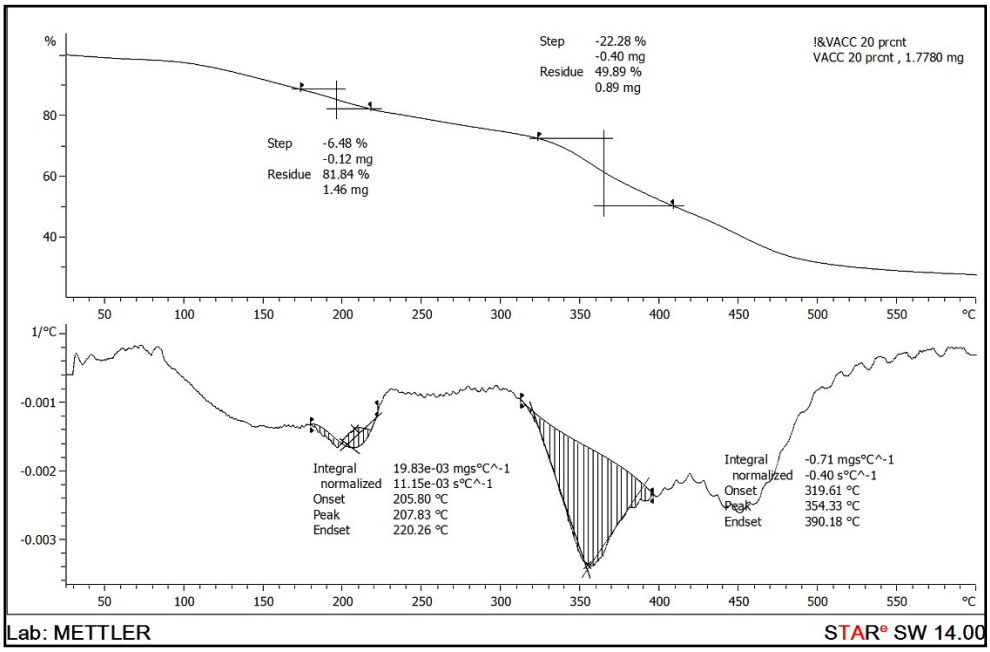

Fig. S2 (e) Thermal analysis plot for compound **3**.

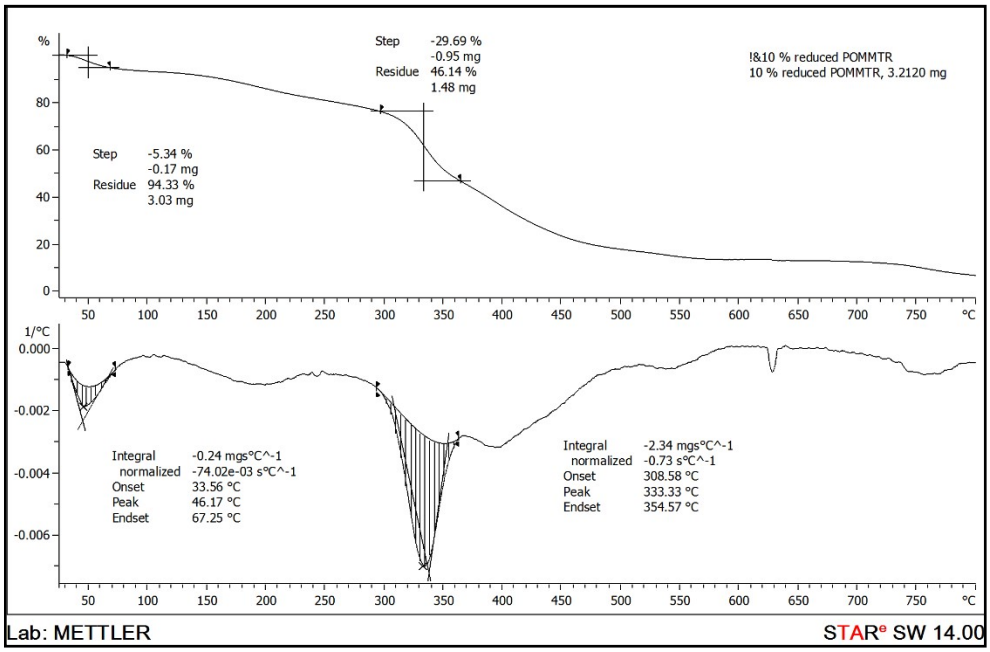

Fig. S2 (f) Thermal analysis plot for compound $\mathbf{1}_{red}$.

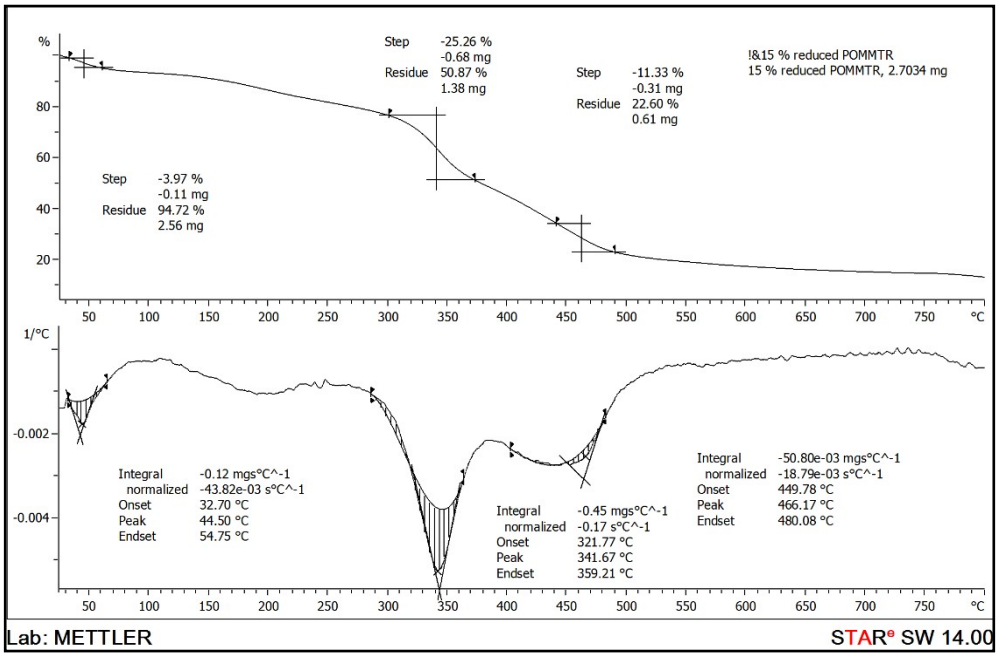

Fig. S2 (g) Thermal analysis plot for compound $\mathbf{2_{red}}$.

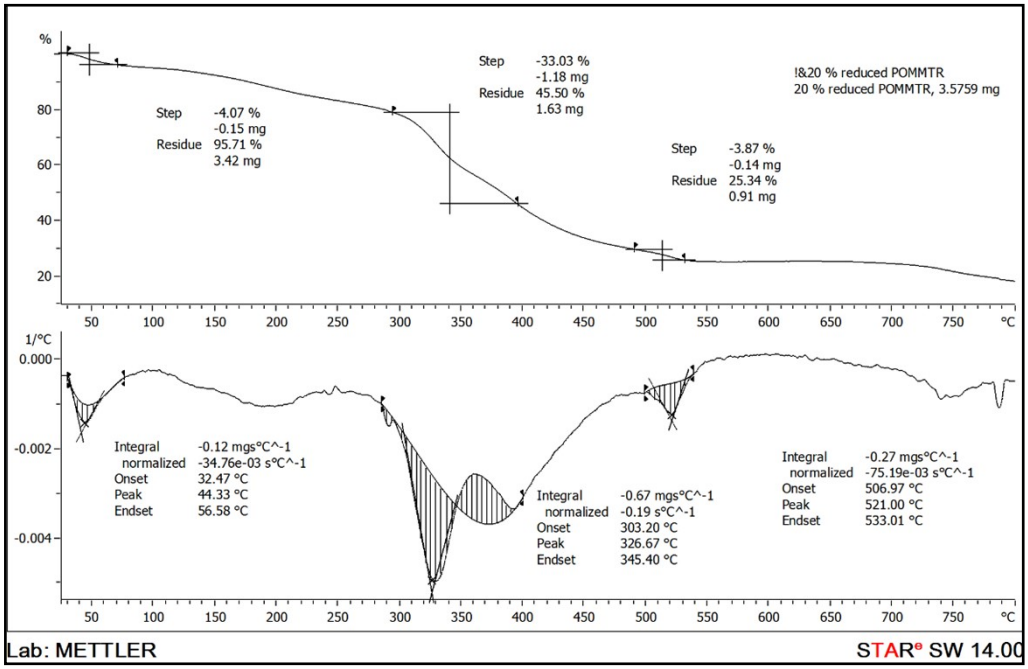

Fig. S2 (h) Thermal analysis plot for compound $\mathbf{3_{red}}$.

5. Scanning electron microscopy

The SEM images of all the compounds are given below (Figure S3(a) to S3(e)). The analysis of the images show that the shape and morphology of the particles are maintained throughout the photo-redox process. The particles are spherical in morphology. The particle sizesare in the range of 30 to 100 nm. The particles in compounds **1**, **2** and **3** show aggregation to some extent in comparison to MTR and PMTR.

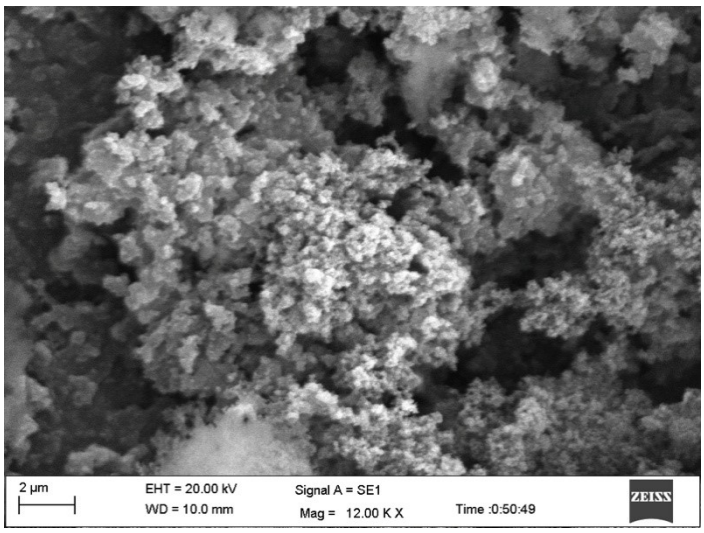

Fig. S3 (a) SEM image of MTR.

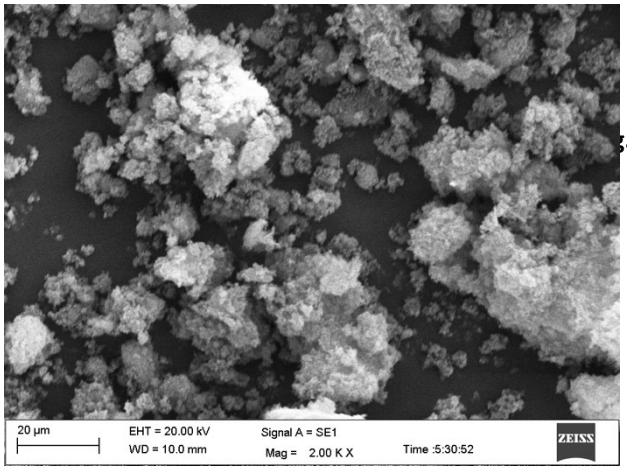
20 µm
EHT = 20.00 kV
WD = 10.0 mm
Signal A = SE1
Mag = 2.00 K X
Time :5:30:52
ZEISS

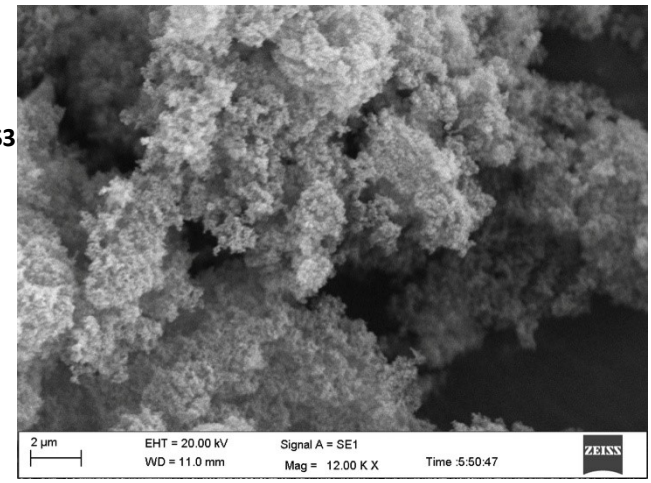
2 µm
EHT = 20.00 kV
WD = 11.0 mm
Signal A = SE1
Mag = 12.00 K X
Time :5:50:47
ZEISS

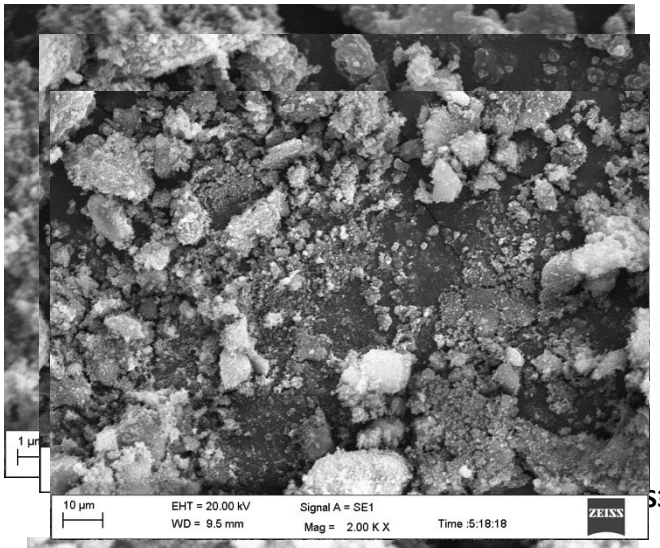
10 µm
EHT = 20.00 kV
WD = 9.5 mm
Signal A = SE1
Mag = 2.00 K X
Time :5:18:18
ZEISS

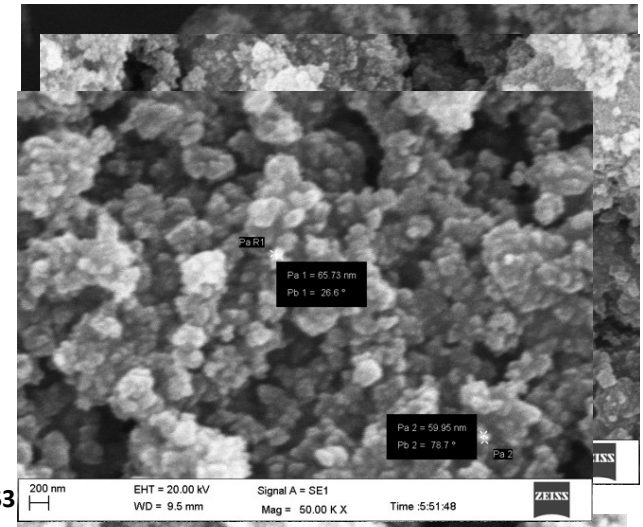
Pa R1
Pa 1 = 65.73 nm
Pb 1 = 26.6 °
Pa 2 = 59.95 nm
Pb 2 = 78.7 °
Pa 2
200 nm
EHT = 20.00 kV
WD = 9.5 mm
Signal A = SE1
Mag = 50.00 K X
Time :5:51:48
ZEISS

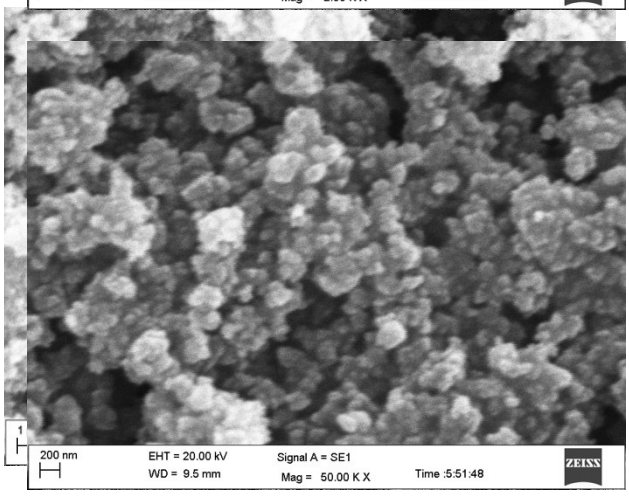
200 nm
EHT = 20.00 kV
WD = 9.5 mm
Signal A = SE1
Mag = 50.00 K X
Time :5:51:48
ZEISS

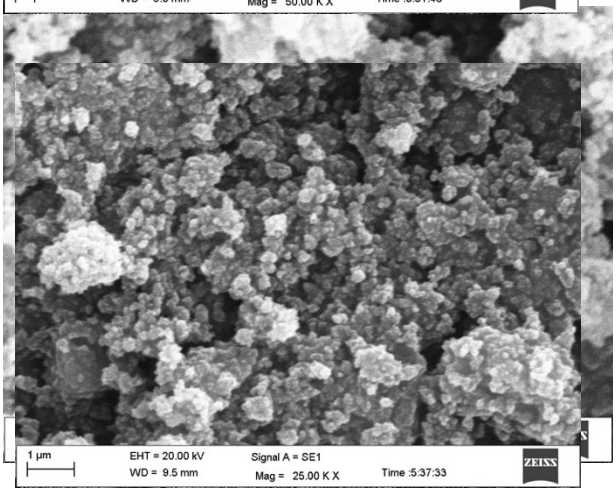
1 µm
EHT = 20.00 kV
WD = 9.5 mm
Signal A = SE1
Mag = 25.00 K X
Time :5:37:33
ZEISS

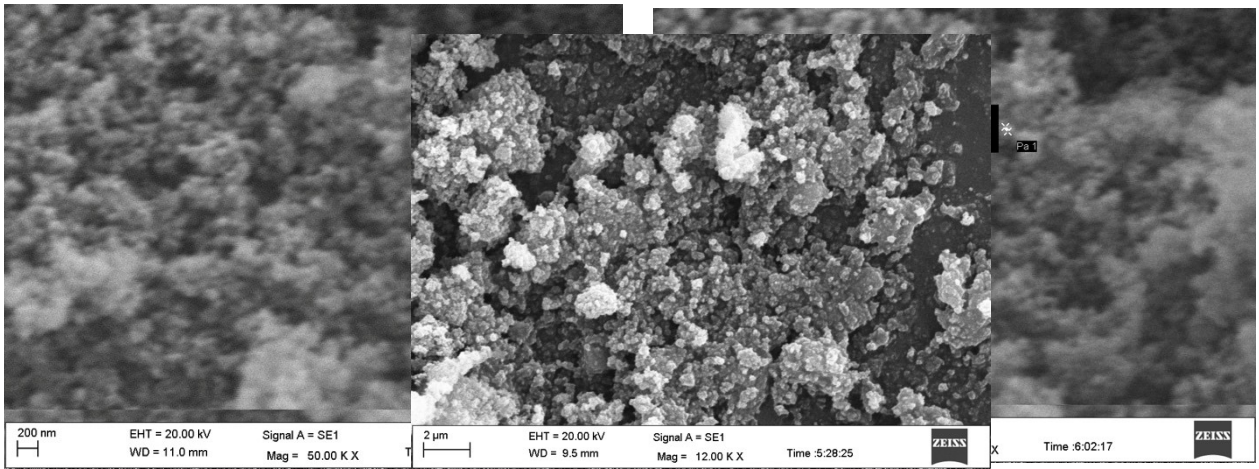
200 nm
EHT = 20.00 kV
WD = 11.0 mm
Signal A = SE1
Mag = 50.00 K X
2 µm
EHT = 20.00 kV
WD = 9.5 mm
Signal A = SE1
Mag = 12.00 K X
Time :5:28:25
ZEISS
Pa 1
Time :6:02:17
ZEISS

Fig. S3 (d). SEM images of compound **2**.

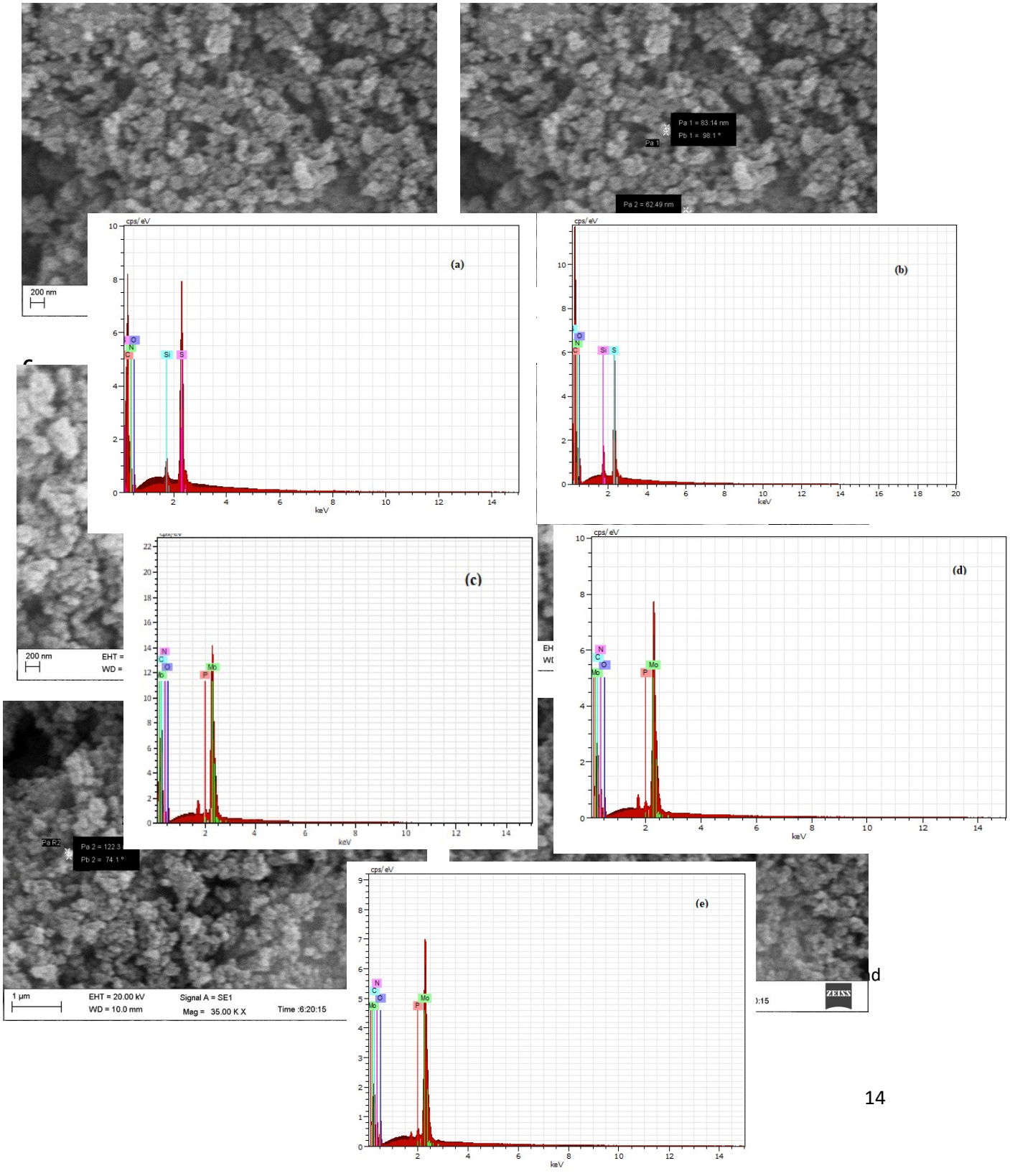

7. BET data

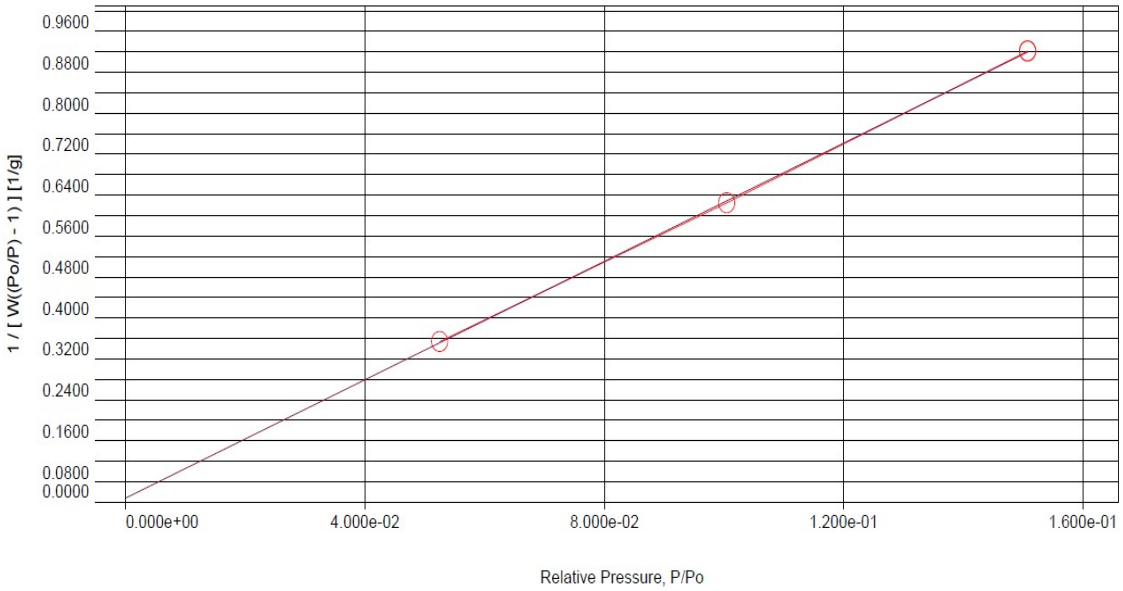

Fig. S5 (a) BET surface area plot for MTR, Correlation coefficient: 0.9999.

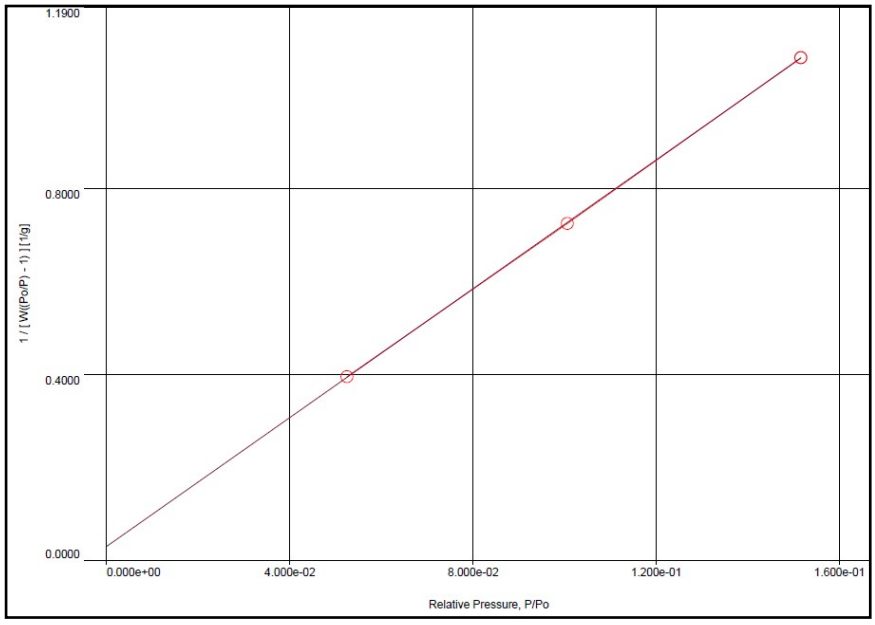

Fig. S5 (b) BET surface area plot for PMTR, Correlation coefficient: 0.9999.

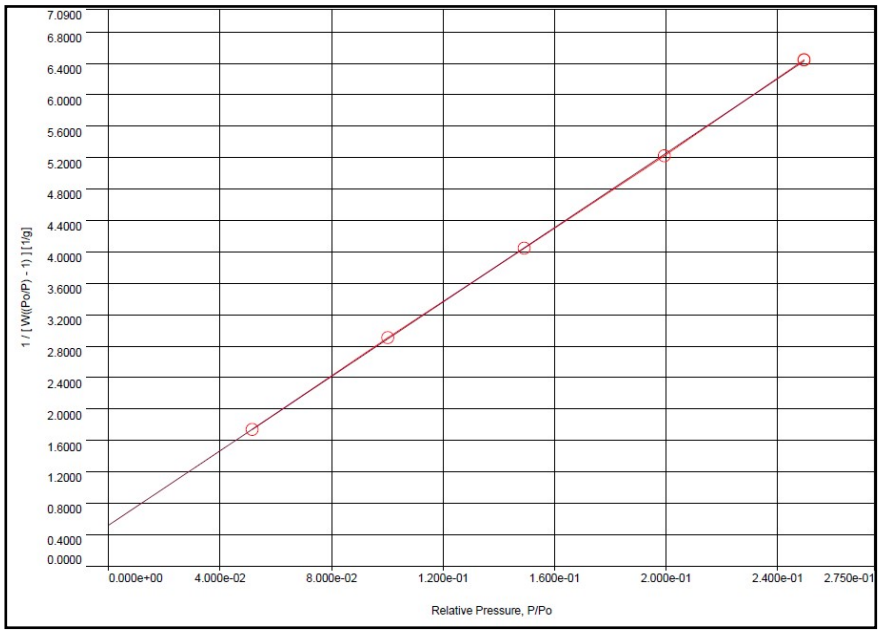

Fig. S5 (c) BET surface area plot for Compound **1**, Correlation coefficient: 0.9999.

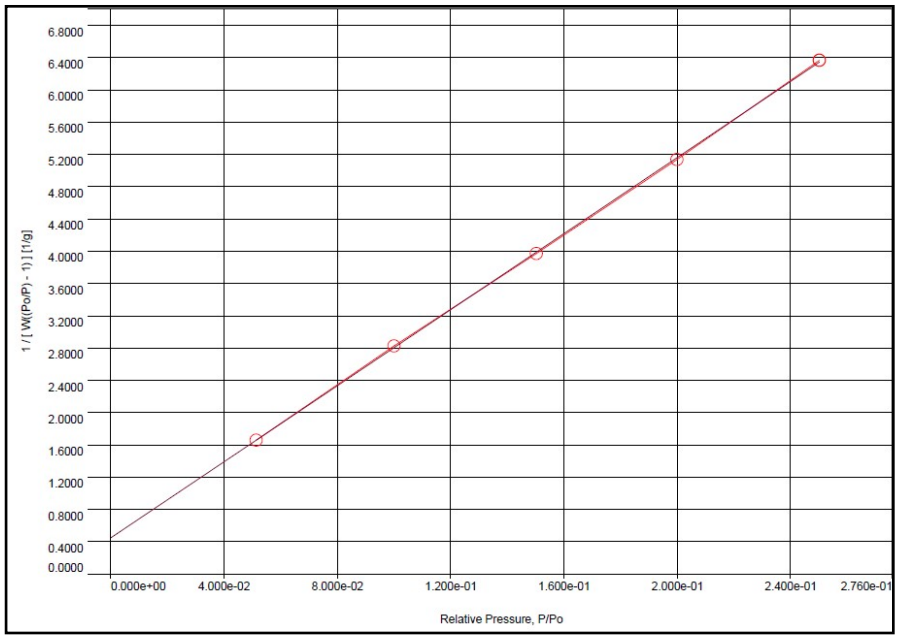

Fig. S5 (d) BET surface area plot for Compound **2**, Correlation coefficient: 0.9999.

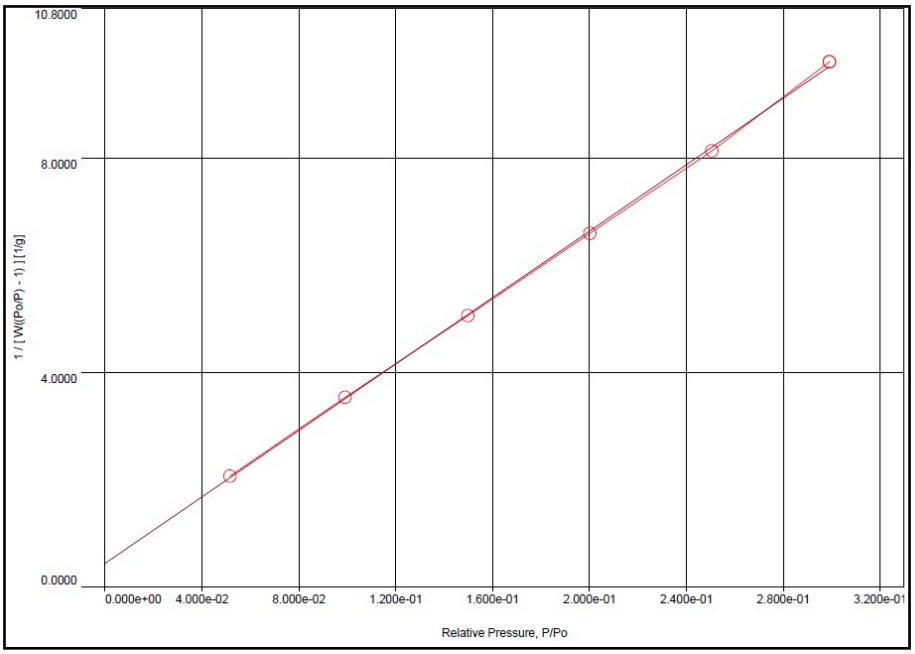

Fig. S5 (e) BET surface area plot for Compound **3**, Correlation coefficient : 0.9999.

Table S2: Surface area**,** porosity and N_2, H_2 and CO_2 adsorption data for POM@PMTR composites.

	Materials	**SA_{Lan} [$m^2 g^{-1}$] T = 77 K**	**SA_{BET} [$m^2 g^{-1}$] T = 77 K**	**Pore volume [$cm^3 g^{-1}$]**	**Average pore size [nm]**	**N_2 adsorbed [$cm^3 g^{-1}$] T = 77 K**	**CO_2 adsorbed [mmol g^{-1}] T = 298 K**	**H_2 uptake [wt. % T= 77 K**
1.	MTR	823. 34	614.02	0.394	1.281	254.34	1.430	0.71
2.	PMTR	709.621	500.05	0.923	3.68	596.83	1.095	0.685
3.	Compound **1**	217.332	143.89	0.154	2.164	108.65	0.776	0.576
4.	Compound**2**	230.115	142.723	0.154	2.164	99.84	0.818	0.612
5.	Compound**3**	186.307	112.453	0.126	2.276	81.51	0.741	0.460

8. Comparison of gas adsorption data with literature reported system

The nitrogen adsorption studies of compounds **1**, **2** and **3** show decrease in surface area in comparison to those of MTR and PMTR. The nitrogen storage capacity of PMTR is greater than that of MTR, which may be due to its mesoporous nature. The nitrogen storage capacities of compounds **1**, **2** and **3** are compared with those of other reported POM-porous substrate systems in Table S3. The nitrogen adsorption properties of PMTR and MTR are compared with those of organic systems with similar surface area.

Table S3. Summary of porosity measurements for various porous materials and different materials supported polyoxometalates (POMs).

Compound	**BET_{SA}** [m^2g^{-1}]	**Storage conditions** Temp.(K)/Press.(bar)	**N_2 storage** [cm^3g^{-1}]	**Pore vol.** [cm^3g^{-1}]	**Average pore size** [nm]	**Ref.**
JUC-597	1857	77/1.0	~756	-	-	1
MTR	614.02	77/1.0	254.34	0.394	1.281	**This work**
PMTR	500.05	77/1.0	596.83	0.923	3.68	**This work**
HAT-COF	486.15	77/1.0	450	0.708	-	2
$PMoV_2$@UiO-66	251	77/1.0	75	-	0.11	3
WO_xC_y/C-700	213.68	-196 °C/1.0	~180	0.282	5.27	4
NENU-500	195	77/1.0	100	-	-	5
WO_xC_y/C-800	149.5	77/1.0	~120	0.196	5.23	4
Compound-1	143.89	77/1.0	108.65	0.154	2.164	**This work**
Compound-2	142.723	77/1.0	99.84	0.154	2.164	**This work**
PMo/Bz-PN-SiO2	122	77/1.0	-	0.41	13.5	6

α-$H_2W_{12}O_{40}^{6-}$LDH adipate	120	77/1.0	-	-	-	7
Cs-PW HMS	117	77/1.0	~110	-	-	8
Compound-3	112.453	77/1.0	81.51	0.126	2.276	**This work**
$Co_4(H_2O)_2(PW_9O_{34})_2^{10-}$LDH adipate	112	77/1.0	-	-	-	7
SiO2@C-dots/QPW5501	109.5	77/1.0	325	-	27.2	9
α-$P_2W_{18}O_6^{26-}$LDH adipate	99	77/1.0	-	-	-	7
SiW_{11}-SiO_2	98.9	77/1.0	-	-	-	10
BW_{11}-SiO_2	91.8	77/1.0	-	-	-	10
SiW_{11}Ni-APS-SiO_2	91.6	77/1.0	-	0.11	1.20	11
PA-1	84.5	77/1.0	~260	0.41	13.6	12
SiW_{11}Ni-APS-SiO-6	83.7	77/1.0		0.43	27.3	11
PW_{11}-SiO_2	81	-	-	-	-	10
Macroporous silica grafted and impregnated with $K_5[CoPW_{11}]$	76	77/1.0	-	0.20	-	13
SiW_{11}Ni-APS-SiO-7	73.9	77/1.0	-	0.19	42.6	11
Mg3-Al-ILs-C_8-LaW10	63	77/1.0	-	0.65	5.87	14
WO_x/C_y/C-900	52.3	-196 ^{O}C/1.0	~70	0.107	5.21	4
1-POM	51	77/1.0	-	-	3.6	15
$[\{Zn(eim)_2 \cdot H_2O\}_\infty]$	28.7	77/1.0	-	-	-	16
2-POM	27	77/1.0	-	-	3.6	15
GeW_{11}-SiO_2	25.8	77/1.0	-	-	-	10
HPW-HSM	17	77/1.0	~18	-	-	8
EB-COFPW$_{12}$	8	77/1.0	~22	-	-	17
$[Cu_{12}(BTC)_8][H_3PW_{12}O_{40}]$	-	77/1.0	142	-	-	18

The hydrogen adsorption data of MTR, PMTR, compounds **1**, **2** and **3** along with other reported systems are summarized in Table S4. The MTR and PMTR materials show better hydrogen storage ability in comparison to that of POM composite materials. There is not much difference in hydrogen adsorption change on protonation. The hydrogen storage of MTR and PMTR porous organic substances are compared with other porous organic materials. The surface area to H_2 storage of MTR and PMTR are in the range of relevant literature values. The hydrogen storage of POM-PMTR composites decreases with increase in POM loading.

Table S4. H_2 storage data of different materials supported polyoxometalates (POMs) and other porous materials.

Compound	**BET area** (m^2g^{-1})	**Storage conditions** Temp.(K)/Press.(bar)	**H_2 storage** (cm^3g^{-1})	**H_2 storage** (wt%)	**Ref.**
JUC-597	1857	77/1.0	148	1.32	1
CTC-COF	1710	77/1.0	125	1.12	19
COF-5	1590	77/1.0	~112	~1	20
COF-105	-	-	-	0.8	21
MTR	614.02	77/1.0	78.82	0.71	**This work**
PMTR	500.05	77/1.0	75.98	0.685	**This work**
Compound-2	142.723	77/1.0	68.09	0.612	**This work**
$CoW_{12}P$-DMF	-	77/1.0	-	~0.61	22
MOF-14	-	-	-	0.6	21
Compound-1	143.89	77/1.0	64	0.576	**This work**
$CoMo_{12}P$-DMF	-	77/1.0	-	~0.57	22
PAF-19	250	77/1.0	62	0.55	23
Compound-3	112.453	77/1.0	51.20	0.46	**This work**
$Zn_4(TRZ)_4$(1,4-BDC)	170	77/1.0	48	0.43	24
$CoW_{12}P$-DEF	-	77/1.0	-	0.4	22

The CO_2 adsorption data for all the compounds are given in Table S5. The porous organic MTR and PMTR exhibit better adsorption properties than POM-PMTR composite material. The adsorption properties of POM composites are comparable to those of some of the reported POM materials. The MTR and PMTR porous organic substances exhibit interesting H_2 and CO_2 adsorption properties in comparison to their POM composite materials.

Table S5. CO_2 adsorption data of different materials supported polyoxometalates (POMs) and other porousmaterials.

Compound	**BET area** (m^2g^{-1})	**Storage conditions** Temp.(K)/Press.(bar)	**CO_2 uptake** (cm^3g^{-1})	**Ref.**
HP-COF-1	1197	273/1.0 atm	54	25
HP-COF-2	804	273/1.0 atm	37	25
MTR	614.02	298/1.0	32.12	**This work**
JUC-597	1857	298/1.0	31	1
$MnMo_6$@TCOF	-	298/1.0	27	26
MnMo6@ECOF	-	298/1.0	26.91	26
PMTR	500.05	298/1.0	24.59	**This work**
Compound-2	142.723	298/1.0	18.40	**This work**
Compound-1	143.89	298/1.1	17.44	**This work**
Compound-3	112.453	298/1.0	16.75	**This work**
CoMo12P-DMF	-	298/1.0	6.5	22
CoW_{12}Si-DEF	-	298/1.0	6.0	22
$CoMo_{12}$P-DEF	-	298/1.0	2.5	22
PA-1	-	298/1.0	1.98	12

9. DFT calculation with ORCA

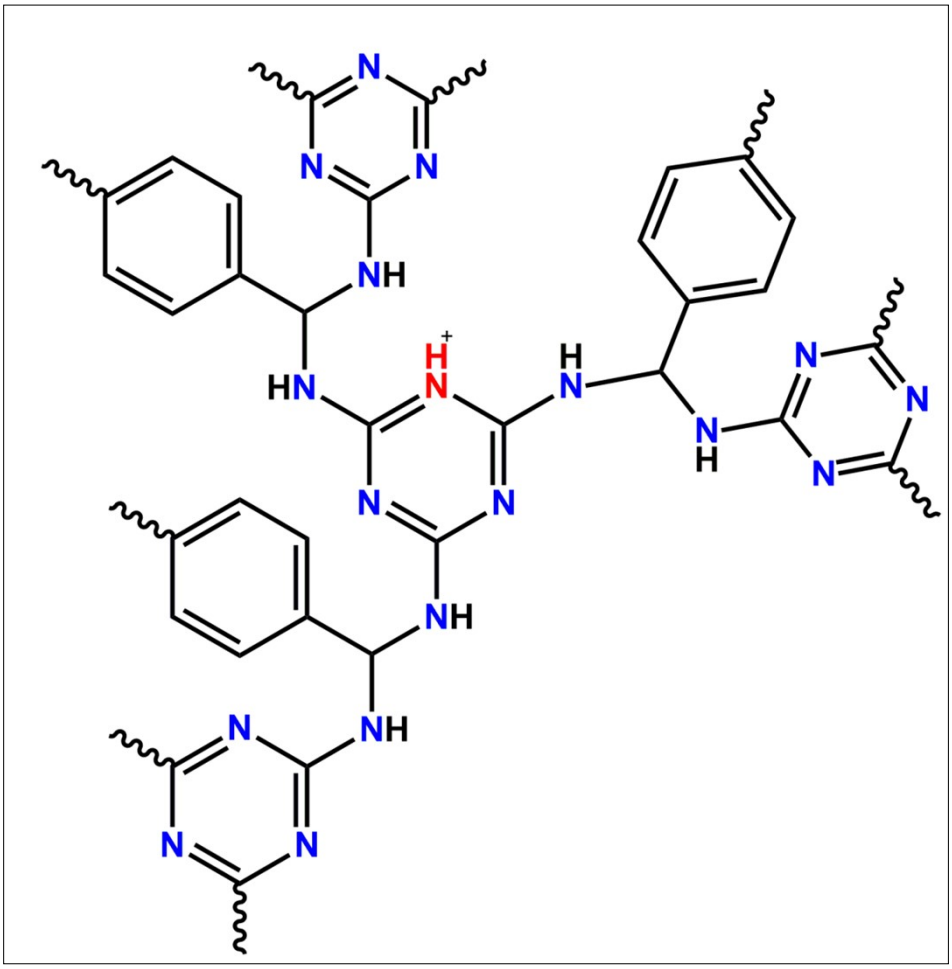

Structure 1: FINAL single point energy **(-2613.921159754852 Hartree).**

All the structures were optimized using Orca version 5.0.1.[27-29] The DFT calculations were carried out using the BP86 functional [30-31] with the Karlsruhe valence triple-zeta basis set "def2-TZVP"[32-34] and Weigend's auxiliary basis set.[35] Dispersion effects were considered by Grimme approximation 'D3'.[36-37]

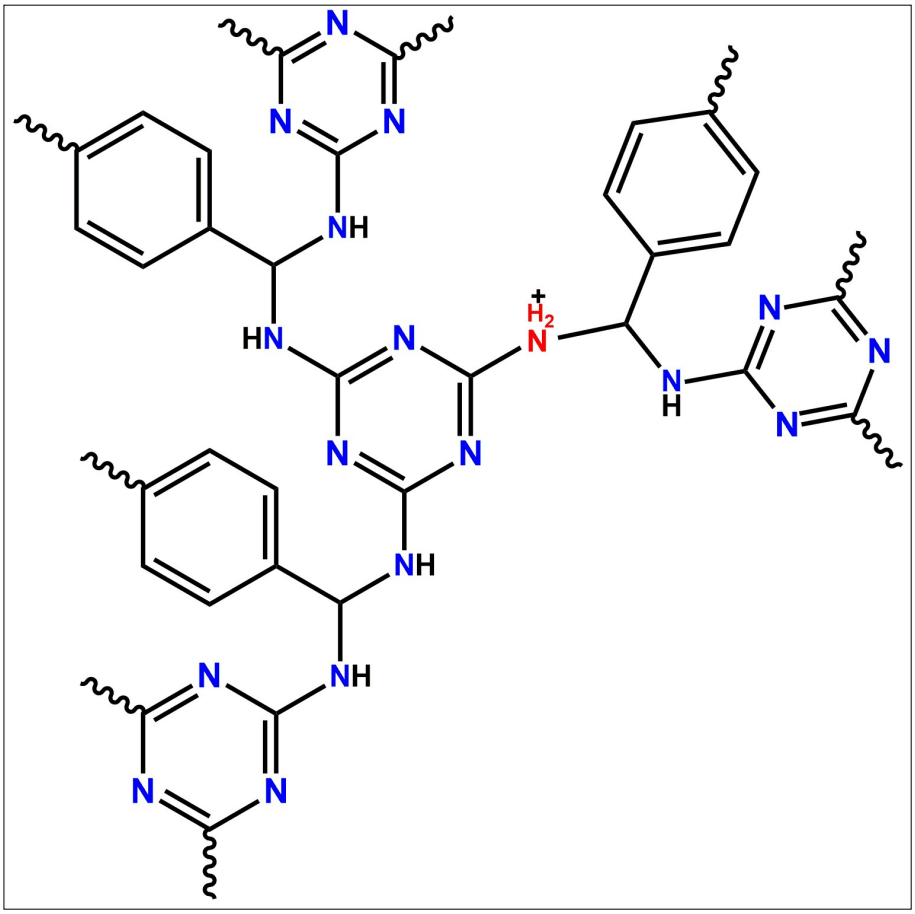

Structure 2: FINAL single point energy **(-2613.907715044699 Hartree**).

The DFT calculations suggested that the protonation on triazinenitrogen of melamine has a lowered single point energy as compared to other protonation site which is on NH. Therefore, structure **1** is more feasible and protonation at triazine ring nitrogen seems to be more favorable.

Table S6. Coordinates for Structure **1**: (Protonation on triazine Nitrogen of melamine)

N	-1.82606	0.16934	-0.46247
C	-1.34116	-1.05955	-0.67196
N	-2.00618	-1.98566	-1.42668
N	-0.12316	-1.39806	-0.27397
C	0.64434	-0.5082	0.33965
N	1.97622	-0.8528	0.59704
N	0.16351	0.69014	0.62776
C	-1.04671	1.03622	0.20437
N	-1.3865	2.35564	0.34111
N	-3.99689	2.17164	3.64007
C	-3.76333	1.90217	2.36589
N	-3.09204	2.89748	1.67962
N	-4.03785	0.73328	1.78879
C	-4.69694	-0.14231	2.55838
N	-4.91957	0.01763	3.85719
C	-4.55983	1.19742	4.357
C	-2.79865	2.70376	0.29467
C	-2.9813	4.00589	-0.47667
C	-4.24939	4.31097	-1.00297
C	-4.4572	5.46664	-1.76304
C	-3.40901	6.36041	-1.99748
C	-2.14922	6.07865	-1.46498
C	-1.94004	4.92359	-0.70486
N	-7.44677	-4.71176	-1.67201
C	-6.39724	-5.42118	-2.07869
N	-5.17961	-4.91171	-2.27519
C	-5.03182	-3.6307	-1.97016
N	-3.74478	-3.14869	-2.1363
N	-6.00027	-2.85138	-1.50728
C	-7.20688	-3.42503	-1.43206
C	-3.43973	-1.84688	-1.64388
C	-3.77224	-0.71276	-2.58817
C	-3.02976	-0.42918	-3.74454
C	-3.31506	0.70791	-4.51019
C	-4.3629	1.56592	-4.15489
C	-5.12983	1.26778	-3.02809
C	-4.84013	0.14205	-2.25776
N	3.88625	1.453	4.03678
C	3.81139	1.37726	2.71656
N	3.0019	0.35028	2.232
N	4.41367	2.20602	1.87629
C	5.23152	3.09931	2.44442
N	5.35947	3.27042	3.75755

C	4.65788	2.43333	4.51773
C	3.01337	0.15847	0.82844
C	4.23529	-0.36456	0.12591
C	4.4455	0.06295	-1.20167
C	5.46298	-0.47724	-1.98209
C	6.30569	-1.45282	-1.4517
C	6.1069	-1.88437	-0.13342
C	5.08184	-1.34504	0.65376
C	7.3737	-2.06232	-2.31343
C	-3.61954	7.57358	-2.85715
C	-4.63914	2.80691	-4.95461
C	4.67748	2.65827	5.99874
C	6.12012	3.91103	1.55376
C	-5.18801	-1.40829	1.92707
C	-4.69809	1.40474	5.8329
C	-8.38419	-2.55668	-1.11296
C	-6.56583	-6.90181	-2.22299
H	-1.84696	-2.97306	-1.26045
H	2.34374	-1.78592	0.42025
H	-3.51646	3.78776	1.93284
H	-3.41874	1.95216	-0.20822
H	-5.09315	3.64184	-0.8422
H	-5.44497	5.66722	-2.176
H	-1.31963	6.76172	-1.64213
H	-0.94118	4.75892	-0.31244
H	-3.49759	-3.33502	-3.10214
H	-3.90392	-1.67971	-0.66443
H	-2.21429	-1.07598	-4.05809
H	-2.72034	0.92338	-5.39702
H	-5.96268	1.90944	-2.74557
H	-5.46069	-0.05869	-1.38533
H	3.25054	-0.44754	2.812
H	2.70019	1.08353	0.32504
H	3.81594	0.82796	-1.65276
H	5.60023	-0.13007	-3.0054
H	6.76067	-2.64786	0.28775
H	4.96385	-1.71038	1.67108
H	7.73576	-1.33903	-3.05253
H	6.97214	-2.93209	-2.84279
H	8.23315	-2.37308	-1.71219
H	-4.6139	8.00022	-2.6907
H	-3.51872	7.30434	-3.91334
H	-2.88688	8.35359	-2.624
H	-4.61533	2.58746	-6.02651
H	-3.89141	3.57299	-4.72584

H	-5.62935	3.21534	-4.72493
H	5.6451	3.05829	6.31676
H	4.49569	1.72347	6.53694
H	3.89653	3.37633	6.26825
H	7.14712	3.53894	1.62721
H	6.10252	4.96256	1.85338
H	5.79954	3.83873	0.51027
H	-5.70982	-1.18126	0.99285
H	-5.88663	-1.93235	2.58656
H	-4.34409	-2.07068	1.71523
H	-5.47717	0.75684	6.2452
H	-4.95667	2.44437	6.05239
H	-3.74887	1.16563	6.3228
H	-8.06222	-1.59097	-0.71225
H	-9.02752	-3.04361	-0.37445
H	-8.96442	-2.37907	-2.02412
H	-7.59296	-7.15181	-2.50355
H	-6.33492	-7.38611	-1.26865
H	-5.88984	-7.29605	-2.98743
H	-1.02165	2.84525	1.15168
H	0.24096	-2.30509	-0.5292

Table S7. Coordinates for Structure **2**: (protonation on triazine Nitrogen of melamine)

N	-1.75455	0.17355	-0.53582
C	-1.26413	-1.03464	-0.74664
N	-1.93018	-1.93469	-1.54313
N	-0.0792	-1.42374	-0.30024
C	0.63411	-0.54466	0.38298
N	1.89137	-0.95049	0.77414
N	0.19785	0.66927	0.66794
C	-1.0024	0.94605	0.20895
N	-1.3098	2.32146	0.31197
N	-3.9903	2.2354	3.65896
C	-3.68481	1.93333	2.40746
N	-2.94739	2.89946	1.73663
N	-3.98072	0.77912	1.82084
C	-4.66572	-0.09121	2.57479
N	-4.97358	0.10238	3.8531
C	-4.60886	1.27888	4.35683
C	-2.7133	2.69006	0.34324
C	-2.95178	3.99931	-0.41159
C	-4.20783	4.23001	-0.99759
C	-4.44604	5.37972	-1.7567
C	-3.44075	6.3337	-1.93794
C	-2.19793	6.13026	-1.33528
C	-1.96255	4.99217	-0.55905
N	-7.45208	-4.67936	-1.67282
C	-6.41714	-5.37216	-2.14268

N	-5.2008	-4.86435	-2.34426
C	-5.02419	-3.60442	-1.9663
N	-3.74551	-3.13255	-2.11696
N	-5.97919	-2.84341	-1.44278
C	-7.18724	-3.41097	-1.36691
C	-3.36632	-1.84029	-1.6544
C	-3.76326	-0.71562	-2.60148
C	-3.03603	-0.43339	-3.76933
C	-3.34002	0.68678	-4.5476
C	-4.39673	1.533	-4.19491
C	-5.15525	1.2345	-3.05981
C	-4.84299	0.123	-2.27321
N	3.98632	1.41269	4.02082
C	3.89539	1.33299	2.69891
N	3.12432	0.31189	2.22904
N	4.47288	2.18406	1.85904
C	5.23994	3.11941	2.4248
N	5.37811	3.29567	3.73808
C	4.72547	2.41608	4.49548
C	2.92305	0.06296	0.84312
C	4.15007	-0.45584	0.106
C	4.3935	-0.01347	-1.20805
C	5.46209	-0.51782	-1.95152
C	6.31744	-1.47351	-1.39815
C	6.07963	-1.92493	-0.09471
C	5.00871	-1.42147	0.65156
C	7.42987	-2.05745	-2.21911
C	-3.68003	7.53436	-2.80773
C	-4.67751	2.7641	-5.00587
C	4.76484	2.60938	5.97928
C	6.05125	3.99836	1.52507
C	-5.10194	-1.37869	1.94645
C	-4.8128	1.50119	5.82327
C	-8.34489	-2.54937	-0.96923
C	-6.60437	-6.84023	-2.36815
H	-1.63106	-2.87387	-1.31101
H	2.15098	-1.76698	0.22984
H	-3.35572	3.79394	2.00446
H	-3.32792	1.92504	-0.14579
H	-5.01759	3.50995	-0.88541
H	-5.42334	5.52678	-2.21506
H	-1.40318	6.86417	-1.4669
H	-0.98487	4.91238	-0.0889
H	-3.34066	-3.45619	-2.98191
H	-3.78461	-1.65839	-0.65661
H	-2.20166	-1.0685	-4.06152
H	-2.74349	0.89597	-5.43378
H	-5.99776	1.86448	-2.78258
H	-5.44762	-0.08381	-1.39205
H	2.9742	-0.44131	2.87681
H	2.61154	0.99383	0.34821
H	3.74722	0.72924	-1.67062
H	5.62157	-0.16356	-2.96815
H	6.72813	-2.6787	0.34811

H	4.84857	-1.79539	1.66042
H	7.8079	-1.32649	-2.94195
H	7.06851	-2.93556	-2.7636
H	8.27148	-2.35409	-1.58513
H	-4.68576	7.9349	-2.64539
H	-3.56903	7.25998	-3.86159
H	-2.96858	8.33553	-2.5807
H	-4.63837	2.53756	-6.07607
H	-3.93682	3.53697	-4.77572
H	-5.67275	3.16588	-4.78934
H	5.73674	3.00245	6.29167
H	4.59222	1.66207	6.49905
H	3.98575	3.31836	6.27608
H	7.09652	3.67444	1.54377
H	5.99794	5.03862	1.85937
H	5.6888	3.94607	0.4941
H	-5.62208	-1.17589	1.00596
H	-5.78739	-1.92502	2.602
H	-4.2319	-2.01044	1.74779
H	-5.6139	0.86206	6.2069
H	-5.07456	2.54411	6.02227
H	-3.88877	1.26012	6.3583
H	-8.00207	-1.6025	-0.54175
H	-8.96515	-3.06216	-0.22845
H	-8.95625	-2.33105	-1.85077
H	-7.63373	-7.05937	-2.66636
H	-6.38537	-7.38044	-1.44141
H	-5.93121	-7.20205	-3.15091
H	-0.91749	2.60895	1.20651
H	-0.806	2.75589	-0.4531

References.

1. C. Yu, H. Li, Y. Wang, J. Suo, X. Guan, R. Wang, V. Valtchev, Y. Yan, S. Qiu and Q. Fang, *Angew. Chem. Int. Ed.,* 2022, **61**, e202117101.
2. S.-Q. Xu, T.-G. Zhan, Q. Wen, Z.-F. Pang and X. Zhao, *ACS Macro Lett.,* 2016, **5**, 99-102.
3. J. Sun, H. S. Jena, S. Abednatanzi, Y.-Y. Liu, K. Leus and P. V. D. Voort,*ACS Appl. Mater. Interfaces.,* 2022, **14**, 37681-37688.
4. X. Luo, F. Li, F. Peng, L. Huang, X. Lang and M. Shi, *ACS Appl. Mater. Interfaces*., 2021, **13**, 57803-57813.
5. J.-S. Qin, D.-Y. Du, W. Guan, X.-J. Bo, Y.-F. Li, L.-P. Guo, Z.-M. Su, Y.-Y. Wang, Y.-Q. Lan and H.-C. Zhou, *J. Am. Chem. Soc.,* 2015, **137**, 7169-7177.
6. M. Craven, D. Xiao, C.-K. Olsen, E.F. Kozhevnikova, F. Blanc, A. Steiner and I. V. Kozhevnikov, *Applied Catalysis B: Environmental.,* 2018, **234**, 247-259.
7. S. K. Yun and T. J. Pinnavaia, *Inorg. Chem.,* 1996, **35**, 6853-6860.
8. T. Okada, K. Miyamoto, T. Sakai and S. Mishima, *ACS Catal.,* 2014, **4**, 73-78.

9. J. Song, Y. Li, P. Cao, X. Jing, M. Faheem, Y. Matsuo, Y. Zhu, Y. Tian, X. Wang and G. Zhu, *Adv. Mater.,* 2019, **31**, e1902444.
10. Y. Guo, Y. Yang, C. Hu, C. Guo, E. Wang, Y. Zou and S. Feng, *J. Mater. Chem*., 2002, **12**, 3046–3052.
11. Y. Guo, C. Hu, C. Jiang, Y. Yang and E. Wang, *Journal of Catalysis*., 2003, **217**, 141–151.
12. S. Zulfiqar, M. I. Sarwar and C. T. Yavuz, *RSC Adv.* **2014,** 4, 52263–52269.
13. B. J. S. Johnson and A. Stein,*Inorg. Chem.,* 2001, **40**, 801-808.
14. T. Li, Z. Wang, W. Chen, H. N. Miras and Y.-F. Song, *Chemistry A European Journal.,* 2017, **23**, 1069-1077.
15. M. V. Vasylyev and R. Neumann, *J. AM. CHEM. SOC.,* 2004, **126**, 884-890.
16. X.-C. Haung, Y.-Y. Lin, J.-P. Zhang and X.-M. Chen, *Angew.chem.,* 2006, **118**, 1887-1889.
17. H. Ma, B. Liu, B. Li, L. Zhang, Y.-G. Li, H.-Q. Tan, H.-Y. Zang and G. Zhu, *J. Am. Chem. Soc.,* 2016, **138**, 5897 -5903.
18. C.-Y. Sun, S.-X. Liu, D.-D Liang, K.-Z. Shao, Y.-H. Re and Z.-M. Su, *J. Am. Chem. Soc.,* 2009, **131**, 5, 1883–1888.
19. J.-T. Yu, Z. Chen, J. Sun, J. Z.-T. Huang and Q.-Y. Zheng, *J. Mater. Chem.,* 2012, **22**, 5369-5373.
20. H. Furukawa and O. M. Yaghi, *J. AM. CHEM. SOC.,* 2009, **131**, 8875–8883.
21. Y.-J. Choi, J.-W. Lee, J.-H. Choi and J.-K. Kang, *Appl. Phys. Lett.,*2008, **92**, 173102.
22. C. Dey, R. Das, P. Pachfule, P. Poddar and R. Banerjee, *Crystal Growth & Design., 2011*, **11**, 139-146.
23. Z. Yan, H. Ren, H. Ma, R. Yuan, Y. Yuan, X. Zou, F. Sun and G. Zhu, *Micropor. Mesopor. Mat.,* 2013, **173**, 92-98.
24. H. Park, J. F. Britten, U. Mueller, J. Lee, J. Li and J. B. Parise, *Chem. Mater.,* 2007, **19**, 1302-1308.
25. Y. Zhu, S. Wan, Y. Jin and W. Zhang, *J. Am. Chem. Soc.*, 2015, **137**, 13772–13775.
26. M. Lu, M. Zhang, J. Liu, T.-Y. Yu, J.-N. Chang, L.-J. Shang, S.-L. Li and Y.-Q. Lan, *J. Am. Chem. Soc.,* 2022, **144**, 1861-187.
27. F. Neese, *Wiley Interdiscip. Rev.: Comput. Mol. Sci.,* 2012, **2**, 73–78.
28. F. Neese, *WileyInterdiscip. Rev.: Comput. Mol. Sci.,* 2018, **8**, e1327.
29. F. Neese, F. Wennmohs, U. Becker and C. Riplinger, *J. Chem. Phys.,* 2020, **152**, 224108.
30. A. D. Becke, *Phys. Rev. A.,* 1988, **38**, 3098–3100.
31. J. P. Perdew, *Phys. Rev. B: Condens. Matter Mater. Phys,* 1986, **33**, 8822–8824.
32. F. Weigend and R. Ahlrichs, *Phys. Chem. Chem. Phys.,* 2005, **7**, 3297–3305.
33. A. Schafer, H. Horn and R. Ahlrichs, *J. Chem. Phys.,* 1992, **97**, 2571–2577.
34. A. Schafer, C. Huber and R. Ahlrichs, *J. Chem. Phys.,*1994, **100**, 5829–5835.
35. F. Weigend, *Phys. Chem. Chem. Phys.,* 2006, **8**, 1057–1065.
36. S. Grimme, J. Antony, S. Ehrlich and H. A. Krieg, *J. Chem. Phys.*, 2010, **132**, 154104.
37. S. Grimme, S. Ehrlich and L. Goerigk, *J. Comput. Chem.,* 2011, **32**, 1456–1465.